

Andreas Bund

## Application of the quartz crystal microbalance for the investigation of nanotribological processes

Published online: 5 August 2003  
© Springer-Verlag 2003

**Abstract** The electrochemical preparation of copper layers was investigated using a quartz crystal microbalance (QCM) with damping monitoring. The damping increase during the deposition could be separated into two contributions arising from an internal and an external friction process. External friction comes from the coupling of the shear motion of the rough metal surface to the viscous liquid. Internal friction occurred only in the coarse grained layers and can be explained by phonon excitations at the grain boundaries.

**Keywords** Copper layers · Damping monitoring · Grain boundaries · Phonon excitations · Quartz crystal microbalance

### Introduction

By tracking the resonance frequency of a quartz crystal, the areal mass density of a layer at its surface can be monitored in situ and with very high sensitivity (quartz crystal microbalance, QCM) [1]. As the quartz crystal oscillates in a thickness shear mode the tribological behaviour of the layer can be studied if, besides the frequency shift, the damping is also measured [2]. This can be done by measuring the real part of the electrical admittance of the quartz crystal near its resonance frequency [3, 4, 5, 6], in the following called the resonance curve (Fig. 1). The center of the curve lies at the reso-

nance frequency,  $f$ ; its full width at half maximum (FWHM),  $w$ , is proportional to the damping of the quartz crystal. If a smooth rigid layer is deposited on the quartz crystal (e.g. by vacuum evaporation) the resonance curve shifts to lower frequencies but does not change its form (Fig. 1, transition from curve A to B). If the layer dampens the oscillation of the quartz crystal (e.g. a liquid), the resonance curve shifts to lower frequencies and at the same time broadens (Fig. 1, transition from curve A to C). From the shift of the curve a complex frequency shift  $\Delta f^*$  can be defined (Eq. 1), whose real part is the shift of the maximum of the resonance curve and whose imaginary part contains the change of the FWHM [7]:

$$\Delta f^* = (f_{\text{layer}} - f_0) + i/2(w_{\text{layer}} - w_0) \quad (1)$$

The mechanical behaviour of the layer can be described by its mechanical impedance,  $Z_M^*$ , which is directly proportional to  $\Delta f^*$  (Eq. 2) [8]:

$$Z_M^* = (-i\pi Z_Q/f_0)\Delta f^* \quad (2)$$

with  $Z_Q$  the mechanical impedance of the quartz crystal ( $8.849 \times 10^6 \text{ kg m}^{-2} \text{ s}^{-1}$ ) and  $f_0$  the fundamental resonance frequency of the unloaded quartz.

In the simplest case, a smooth rigid layer with density  $\rho$  and thickness  $L$ ,  $Z_M^* = \rho L$ , and the well-established Sauerbrey equation [9] results from Eq. 2. However, electrochemically prepared layers often have a certain surface roughness which strongly depends on the preparation conditions. By applying an in situ combination of AFM and QCM we could show that failure of the Sauerbrey equation is observed in the case of strong surface roughness [10]. It is important to note that the quartz crystal is sensitive to surface roughness features of the order of magnitude of the penetration depth of the viscous shear wave,  $\delta = (\eta_L/\pi f \rho_L)^{0.5}$ , with  $\eta_L$  and  $\rho_L$  the viscosity and density of the contacting fluid, respectively. For a 10 MHz wave in aqueous solutions,  $\delta = 100$ – $200 \text{ nm}$ . The influence of surface roughness on the QCM signal is difficult to model; the best theories available at

Presented at the 3rd International Symposium on Electrochemical Processing of Tailored Materials held at the 53rd Annual Meeting of the International Society of Electrochemistry, 15–20 September 2002, Düsseldorf, Germany

A. Bund  
Institute of Physical Chemistry and Electrochemistry,  
Dresden University of Technology, 01062 Dresden, Germany  
E-mail: andreas.bund@chemie.tu-dresden.de  
Tel.: +49-351-46334351  
Fax: +49-351-46337164

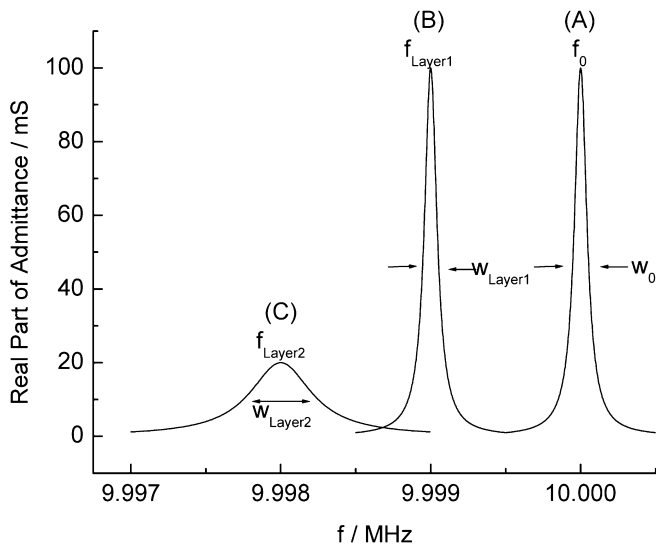


**Fig. 1** Resonance curve of a quartz crystal with different acoustic loads: (A) unloaded quartz; (B) quartz with smooth rigid layer; (C) quartz with damping layer

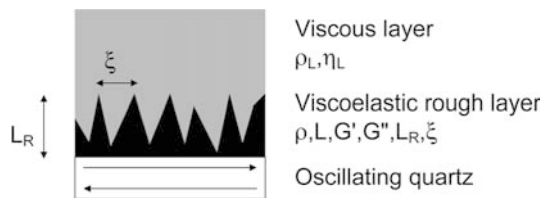


**Fig. 2** Schematic representation of the system quartz + rough viscoelastic layer in a semi-infinite viscous medium

the moment are based on the flow of a viscous medium through a porous layer [11, 12, 13]. These models use two characteristic length scales,  $L_R$  and  $\xi$ , to describe the average surface roughness of the layer in the vertical and the lateral dimensions, respectively (Fig. 2). It is obvious that  $L_R > L$ , indicating the corrugated structure of the surface.

Furthermore, deviation from the Sauerbrey behaviour will be observed if the layer is viscoelastic, as in the case of a polymer layer [14]. In this case the complex frequency shift becomes a function of the thickness  $L$ , the density  $\rho$ , and the complex shear modulus  $G^* = G' + iG''$  of the layer [8].

Recently, we proposed a model to describe the QCM signal of electrochemically prepared layers, being both rough and viscoelastic [15]. The model was applied to study the electropolymerization of thiophenes and the surface roughness data agreed reasonably with the information from scanning electron micrographs. The evaluation procedure, which is described in full detail in [15], models the experimentally observed complex frequency shift ( $\Delta f^*$ , Eq. 3) as the sum of a bulk ( $\Delta f_B^*$ , Eq. 4) and surface roughness contributions ( $\Delta f_R^*$ , Eq. 5):

$$\Delta f^* = \Delta f_B^*(L, \rho, G^*) + \Delta f_R^*(L_R, \xi, \rho_L, \eta_L) \quad (3)$$

$$\Delta f_B^* = -\frac{f_0}{\pi Z_Q} \sqrt{\rho G^*} \tan\left(\sqrt{\rho/G^*} \omega L\right) \quad (4)$$

$$\Delta f_R^* = -\frac{f_0}{\pi Z_Q} \omega \rho_L \left( \frac{1}{q_0} + \frac{L_R}{\xi^2 q_1^2} - \frac{1}{W \xi^2 q_1^2} \right) \times \left\{ \frac{2q_0}{q_1} [\cosh(q_1 L_R) - 1] + \sinh(q_1 L_R) \right\}$$

where  $q_0 = (2\pi i f \rho_L / \eta_L)^{1/2}$ ,  $q_1^2 = q_0^2 + \xi^{-2}$  and  $W = q_1 \cosh(q_1 L_R) + q_0 \sinh(q_1 L_R)$ .

In this paper we apply the evaluation procedure to study the electrodeposition of Cu at different overpotentials.

## Experimental

All solutions were prepared from analytical grade chemicals and highly purified water.

The quartz crystals were optically polished 10 MHz AT cut blanks (diam. 15 mm) with Au electrodes (diam. 5 mm, thickness ca. 100 nm) on a chromium adhesion layer (ca. 5 nm) provided by KVG (Neckarbischofsheim, Germany). They were held between two O-ring gaskets made from Kalrez (Dupont Dow Elastomers, Newark, Del., USA). The quartz was placed at the bottom of a cylindrical PTFE cell (house made). The potential of the Au electrode facing the solution was controlled with an EG the other electrode faced air. The potentials were measured versus a saturated calomel electrode (SCE, Meinsberg Sensortechnik, Meinsberg, Germany). The counter electrode was a copper rod. The reference electrode was placed directly above the quartz to reduce the ohmic drop in the solution and to act as a spoiler for longitudinal waves [16].

The real part of the electrical admittance of the quartz crystal (Fig. 1) was measured with a network analyzer (Advantest R3753BH), transferred to a PC compatible computer via GPIB interface and fit with a Lorentzian. Approximately every 500 ms one dataset could be acquired, consisting of the resonance frequency  $f$ , the FWHM  $w$ , the current, potential and charge.

The data evaluation procedure to extract the bulk and surface roughness parameters from Eqs. 3, 4, 5 was implemented as a Visual C++ program using a Simplex algorithm as described in [17]. It minimizes the squared difference between the measured and calculated complex frequency shifts,  $\chi^2 = (\Delta f_{\text{meas}} - \Delta f_{\text{calc}})^2 + (\Delta w_{\text{meas}} - \Delta w_{\text{calc}})^2$ , where  $\Delta f_{\text{calc}}$  and  $\Delta w_{\text{calc}}$  are obtained from Eqs. 3, 4, 5. If one looks at Eq. 3 there are eight unknowns,  $L$ ,  $\rho$ ,  $G'$ ,  $G''$ ,  $L_R$ ,  $\xi$ ,  $\rho_L$  and  $\eta_L$ , and only two measured quantities,  $\Delta f_{\text{meas}}$  and  $\Delta w_{\text{meas}}$ , and one might argue that the fitting problem is mathematically underdetermined. However, as outlined in [15], one experiment gives  $2N$  data ( $N$  complex frequency shifts coming from  $N+1$  acquired resonance curves), and the description needs only  $N+5$  or  $N+6$  fitting parameters:

1.  $N$  layer thicknesses.
2.  $G'$ ,  $G''$  and  $\xi$  (which are assumed to be constant during the experiment).
3. A two- or three-parameter function  $L_R(L)$  describing the dependence of the vertical dimension of the roughness  $L_R$  on  $L$ . Here, we used an Avrami-type function,  $L_R(L) = L_{R,\text{max}} \{1 - \exp[-k(L/L_{R,\text{max}})^n]\}$ .

For the density of the layer and density and viscosity of the contacting liquid literature data can be used; here  $\rho_L = 998 \text{ kg m}^{-3}$  and  $\eta_L = 1.00 \text{ mPa s}$  [18].

Scanning electron microscopy (SEM) investigations were performed with a Zeiss DSM 982 Gemini microscope (Carl Zeiss, Germany).

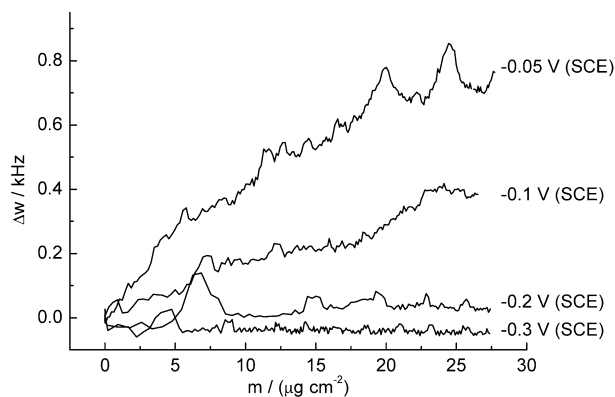


**Fig. 3** Damping increase during potentiostatic Cu deposition from 0.01 M  $\text{CuSO}_4$ , 0.1 M  $\text{Na}_2\text{SO}_4$ , pH 2 for different deposition potentials

## Results and discussion

During the potentiostatic Cu depositions from the acid  $\text{CuSO}_4$  electrolyte, the damping increased during the deposition. The smaller the overpotentials, the higher was the damping increase (Fig. 3). The scanning electron micrographs showed that the damping increase can be correlated with the surface roughness of the layer. At small overpotentials, relatively large grains are formed (Fig. 4a), whereas at more cathodic potentials a dense and finely grained layer is obtained (Fig. 4b). The dependence of the grain size on the polarization is well known [19] and the QCM results are in agreement with published results [10].

Using the evaluation procedure described in [15], the surface roughness parameters (Table 1) could be extracted from the data sets shown in Fig. 3. The layer thickness  $L$ , which would correspond to a smooth layer, lies between 25 and 45 nm. The surface roughness parameters,  $L_R$  and  $\zeta$ , decrease with decreasing deposition potentials. As an example, Fig. 5 shows the measured data (squares) as well as the fit (solid line) and the individual contributions from the bulk and from the surface roughness (dashed lines) for the Cu film deposited at  $-50$  mV (SCE) for ca. 120 s. At such small deposition charges (i.e. layer thicknesses) the damping increase is completely caused by surface roughness effects (Fig. 5b). The surface roughness accounts for ca. 15% of the observed frequency decrease (Fig. 5a). At a first glance one could think that this contribution is caused by liquid molecules which are trapped in surface corrugations and move in phase with the quartz and thus appear as an additional mass. For certain surface morphologies this simple picture may be true [20], but the fact that there is also a damping increase indicates that the situation is more complicated. If only the frequency shift had been monitored and evaluated according to the theory of Sauerbrey, a systematic error of the area mass density of at least 15% would have resulted. The problem

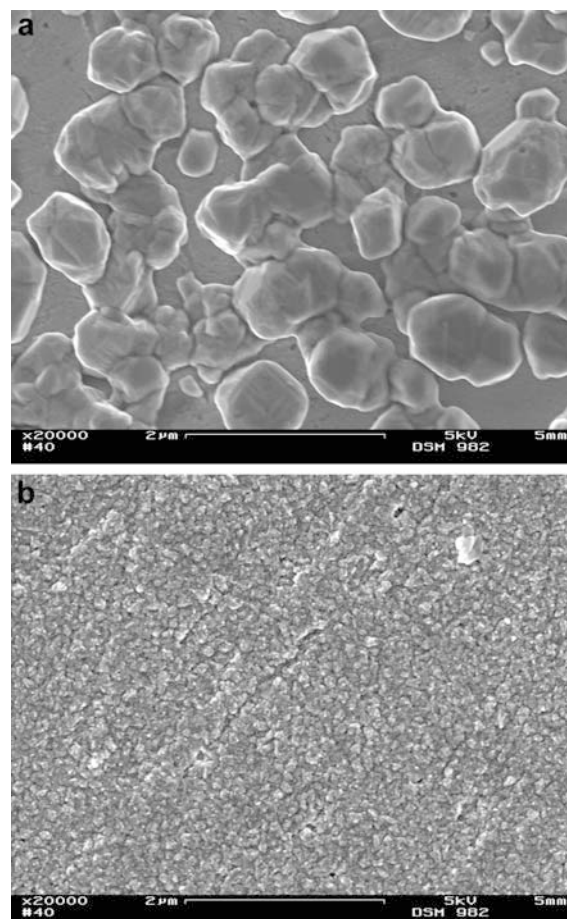


**Fig. 4** SEM micrographs of potentiostatically deposited (a,  $-50$  mV vs. SCE,  $Q = -790$  mC  $\text{cm}^{-2}$ ; b,  $-300$  mV vs. SCE,  $Q = -340$  mC  $\text{cm}^{-2}$ ) Cu layers from 0.01 M  $\text{CuSO}_4$ , 0.1 M  $\text{Na}_2\text{SO}_4$ , pH 2; substrate Au foil

**Table 1** Bulk ( $L$ ,  $G'$ ,  $G''$ ) and surface roughness ( $L_R$ ,  $\zeta$ ) parameters for different Cu layers as determined by the QCM

$E$ vs. SCE (V)	$L$ (nm)	$G'$ (Pa)	$G''$ (Pa)	$L_R$ (nm)	$\zeta$ (nm)
-0.05	25	–	–	160	80
-0.10	34	–	–	120	80
-0.20	45	–	–	10	10
-0.30	30	–	–	0	0
-0.05	140	$10^6$	$10^6$	200	40

becomes worse if the quartz is used as the frequency-controlling element in a feedback oscillator, a measuring technique used relatively often in electrochemical QCM measurements. Depending on the circuitry used, part of the damping change will be “added” to the frequency change and an even larger systematic error results [21].

The  $\Delta f^*$  data for thicker Cu layers (Fig. 6) could only be fit by assuming a storage modulus  $G'$  and a loss modulus  $G''$  of ca.  $10^6$  Pa (Table 1), which is quite unusual for a metal. For bulk copper one would expect a  $G'$  value of the order of GPa and  $G'' = 0$ . Obviously,

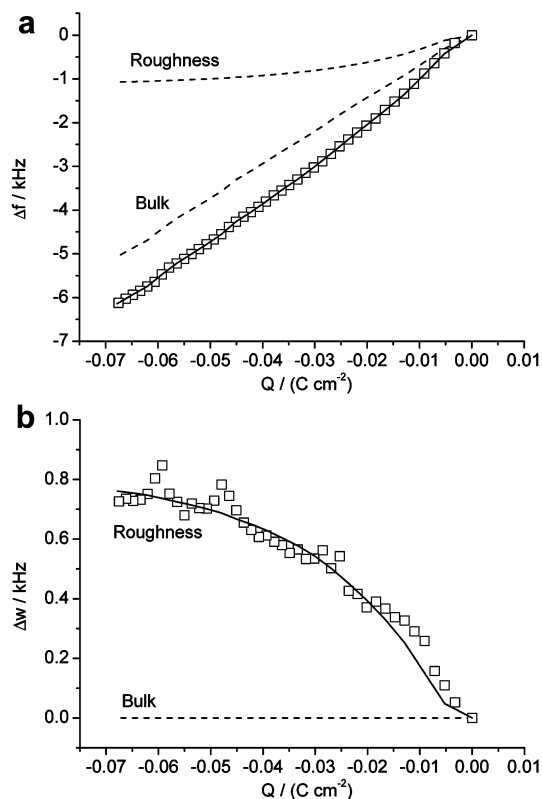


**Fig. 5** Measured (*squares*) and fitted (*full line*) frequency (**a**) and damping (**b**) shifts during the potentiostatic deposition (0.05 V vs. SCE) of ca. 25 nm Cu from 0.01 M CuSO<sub>4</sub>, 0.1 M NaSO<sub>4</sub>, pH 2. *Dashed lines* represent the surface roughness and bulk contribution in the fitted values

there is an energy dissipating effect which becomes active as the deposition charge reaches 0.15 C cm<sup>-2</sup> (Fig. 6b), which corresponds to a mass density of ca. 49  $\mu\text{g cm}^{-2}$  or a layer thickness of ca. 50 nm. In accordance with results from Schumacher [22], this finding can be interpreted with internal wearless friction effects at grain boundaries. As the shear wave travels through a grained material it excites phonons at the grain boundaries, which are the origin of energy dissipation. This mode of energy dissipation becomes active as there are enough grain boundaries touching each other, which explains the existence of a limiting surface coverage seen in Fig. 6b. Fine grained layers such as those shown in Fig. 4b do not show this effect. Therefore, in addition to the critical surface coverage, there seems to be a dependence on the average grain size, which will be the subject for further investigations.

## Conclusions

In conclusion it must be stated that care must be taken when evaluating QCM experiments with rough and/or coarse grained Cu layers. This is especially true if only the frequency shift of the quartz is monitored or, in other words, if one “rides” on the maximum of the

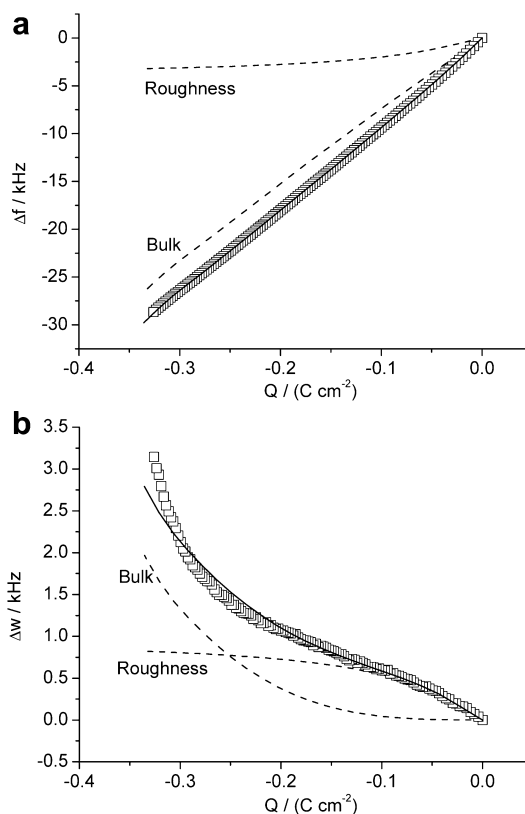


**Fig. 6** Measured (*squares*) and fitted (*full line*) frequency (**a**) and damping (**b**) shifts during the potentiostatic deposition (0.05 V vs. SCE) of ca. 140 nm Cu from 0.01 M CuSO<sub>4</sub>, 0.1 M NaSO<sub>4</sub>, pH 2. *Dashed lines* represent the surface roughness and bulk contribution in the fitted values

resonance curve (Fig. 1). In many QCM experiments, only the frequency shift is monitored and evaluated using the relation of Sauerbrey [9], which is only valid for smooth and rigid layers. In the case of metal layers, one would expect that at least the condition of rigidity is fulfilled. However, our results indicate that metal layers can show some degree of “viscoelasticity”.

**Acknowledgements** Financial support from the “Fonds der Chemischen Industrie” is gratefully acknowledged.

## References

1. Buttry DA, Ward MD (1992) Chem Rev 92:1355
2. Bund A, Schwitzgebel G (2000) Electrochim Acta 45:3703
3. Kipling AL, Thompson M (1990) Anal Chem 62:1514
4. Glidle A, Hillman AR, Bruckenstein S (1991) J Electroanal Chem 318:411
5. Martin SJ, Granstaff VE, Frye GC (1991) Anal Chem 63:2272
6. Schröder J, Borngreber R, Lucklum R, Hauptmann P (2001) Rev Sci Instrum 72:2750
7. Tabidze AA, Kazakov RKH (1983) Meas Technol 14:24
8. Johannsmann D, Mathauer K, Wegner G, Knoll W (1992) Phys Rev B 46:7808
9. Sauerbrey G (1959) Z Phys 155:206

10. Bund A, Schneider O, Dehnke V (2002) *Phys Chem Chem Phys* 4:3552
11. Daikhin L, Urbakh M (1997) *Faraday Discuss* 107:27
12. Daikhin L, Giladi E, Katz G, Tsionsky V, Urbakh M, Zagidulin D (2002) *Anal Chem* 74:554
13. Etchenique R, Brudny VL (2000) *Langmuir* 16:5064
14. Lucklum R, Behling C, Hauptmann P (2000) *Sens Actuators B* 65:277
15. Bund A, Schneider M (2002) *J Electrochem Soc* 149:E331
16. Bund A, Schwitzgebel G (1998) *Anal Chim Acta* 364:189
17. Press WH, Teukolsky SA, Vetterling WT, Flannery BP (1992) *Numerical Recipes in C*, 2nd edn. Cambridge University Press, Cambridge
18. Lide DR (ed) (1999) *CRC handbook of chemistry and physics*, 80th edn. CRC Press, Boca Raton
19. Penner RM (2001) *J Phys Chem B* 105:8672
20. Schumacher R (1990) *Angew Chem* 102:347
21. Fruböse C, Doblhofer K, Soares DM (1993) *Ber Bunsenges Phys Chem* 97:475
22. Küssner T, Wünsche M, Schumacher R (2001) *Surf Sci* 477:102